PERGAMON

Journal of Structural Geology 22 (2000) 1105–1123

JOURNAL OF STRUCTURAL GEOLOGY

www.elsevier.nl/locate/jstrugeo

# The anatomy of shallow-crustal transpressional structures: insights from the Archaean Carajás fault zone, Amazon, Brazil

Robert E. Holdsworth[a,*], Roberto V.L. Pinheiro[a,b]

[a]*Department of Geological Sciences, Reactivation Research Group, University of Durham, South Road Science Laboratories, Durham DH1 3LE, UK*

[b]*Departamento de Geologia, Universidade Federal do Pará, CP 1611, Belém (PA), 66075-900, Brazil*

Received 4 October 1999; accepted 23 February 2000

**Abstract**

The Carajás fault zone (CFZ) is the most prominent structure in the E–W-trending Carajás strike-slip system (CaSSS), an ancient upper crustal fault network of probable Late Archaean age that cuts across the Precambrian Amazonian Craton in Brazil. The subvertical faults reactivated pre-existing, high-grade basement shear-zone fabrics (Itacaiúnas shear zone) and display a complex, long-lived history of movement (>1 Ga) dominated by oblique- and strike-slip displacements. A postulated early regional phase of dextral movement downfaulted units of low-grade to unmetamorphosed basement rocks into dilational bends and offsets in the CaSSS. Subsequent sinistral transpression ca. 2.6 Ga led to faulting and folding during partial inversion of the cover rocks in these dilational sites with much of the associated deformation focused in the immediate vicinity (<2 km) of the major fault traces. The youngest sequence of rocks affected by sinistral transpression along the CFZ—the Águas Claras Formation—were apparently deformed prior to complete lithification and developed a complex assemblage of disharmonic, curvilinear folds and associated transpressional fault arrays. The structures are generally comparable to published descriptions of fold and fault assemblages from shallow-crustal transpressional settings, notably along the San Andreas Fault. However, the meso-scale deformation patterns observed in the Águas Claras road section point to a hitherto unrecognised level of structural complexity that may exist adjacent to comparable transpressional fault zones in many Mesozoic and Cenozoic settings. Our findings suggest that the architecture and underlying dynamic controls of structural development in shallow crustal transpression zones have remained similar for at least the last 2.6 Ga. 

## 1. Introduction

It is generally recognised that Precambrian continental interiors formed by the accretion and reworking of arc terranes brought together by subduction or strike-slip tectonics. In common with many other continental interiors, the South American Platform in Brazil comprises a complex collage of Archaean cratons separated and internally dismembered by a network of regional-scale shear zones or mobile belts. Reactivation of Precambrian basement structures on both regional and local scales during later Archaean to Recent times is widely documented in Brazil (e.g. Le Pichon and Haynes, 1971; Costa et al., 1991, 1993; Pinheiro and Holdsworth, 1997a) and many other continental interiors (e.g. Sutton and Watson, 1986; White et al., 1986; Holdsworth et al., 1997). Many of these reactivated structures are of economic significance as they control the location and architecture of hydrothermal metalliferous ore deposits (e.g. O'Driscoll, 1986) and banded ironstone formations (e.g. Pinheiro and Holdsworth, 1997b). Brittle reactivated structures of Archaean age represent some of the earliest examples of upper crustal tectonic structures formed in continental settings. The present study documents the structural geometry, kinematics and evolution of a well-exposed part of the Carajás fault zone (CFZ; Fig. 1), a

* Corresponding author.
*E-mail address:* R.E.Holdsworth@durham.ac.uk (R.E. Holdsworth).

0191-8141/00/$ - see front matter 
PII: S0191-8141(00)00036-5

structure of probable Late Archaean age in the southern Amazon region of Brazil. This fault zone formed in the upper crust during a long-lived regime dominated by successive phases of transtensional/transpressional displacements. It therefore allows a direct examination of the styles of deformation in a very early example of reactivation and oblique- to strike-slip tectonics in a shallow crustal setting. These structures can also be compared to examples of equivalent deformation features in younger transpressional settings.

## 2. Regional geological framework

### 2.1. General geology and geological history

The Carajás region lies in the southern part of the Amazonian Craton in Brazil. It lies within the E–W-trending Itacaiúnas Belt (Fig. 1) bounded to the east by the Late Proterozoic Araguaia Belt and overlain to the west by a sequence of Mid-Proterozoic cover rocks (Araújo and Maia, 1991). To the south, the Itacaiúnas Belt is in contact with the Archaean Sul do Pará Granite–Greenstone Terrain, whilst to the north, it is covered by Palaeozoic and Cenozoic sediments related to the intracratonic Amazon Basin. The Carajás strike-slip system (CaSSS) is the largest fault system recognised within the Itacaiúnas Belt (Fig. 1). A sub-parallel, probably related, sigmoidal fault array, the Cinzento strike-slip system (CzSSS) lies further to the north. On satellite and radar images (Fig. 2a) the CaSSS and CzSSS collectively form a generally E–W-trending set of discontinuous, sigmoidally shaped, anastomosing lineaments with an along-strike length of almost 200 km and a maximum width of 80 km (see also Figs. 1 and 2b). The CFZ forms the single most prominent structure in the CaSSS, although its lateral terminations extend beyond the zone of sigmoidally shaped lineaments (Pinheiro and Holdsworth, 1997a). A later set of N–S to NNE–SSW-trending fault lineaments cross-cut the main sigmoidal structures (Fig. 2a and b) and are also observed throughout the Amazon Craton.

Much of the Itacaiúnas Belt is dominated by high grade Archaean gneisses referred to as the *Basement Assemblage* (Fig. 2b and c; Pinheiro, 1997; Pinheiro and Holdsworth, 1997a). An older group of granulite facies orthogneisses (Puim Complex; ca. 3.0 Ga) is recognised, together with a younger sequence of upper

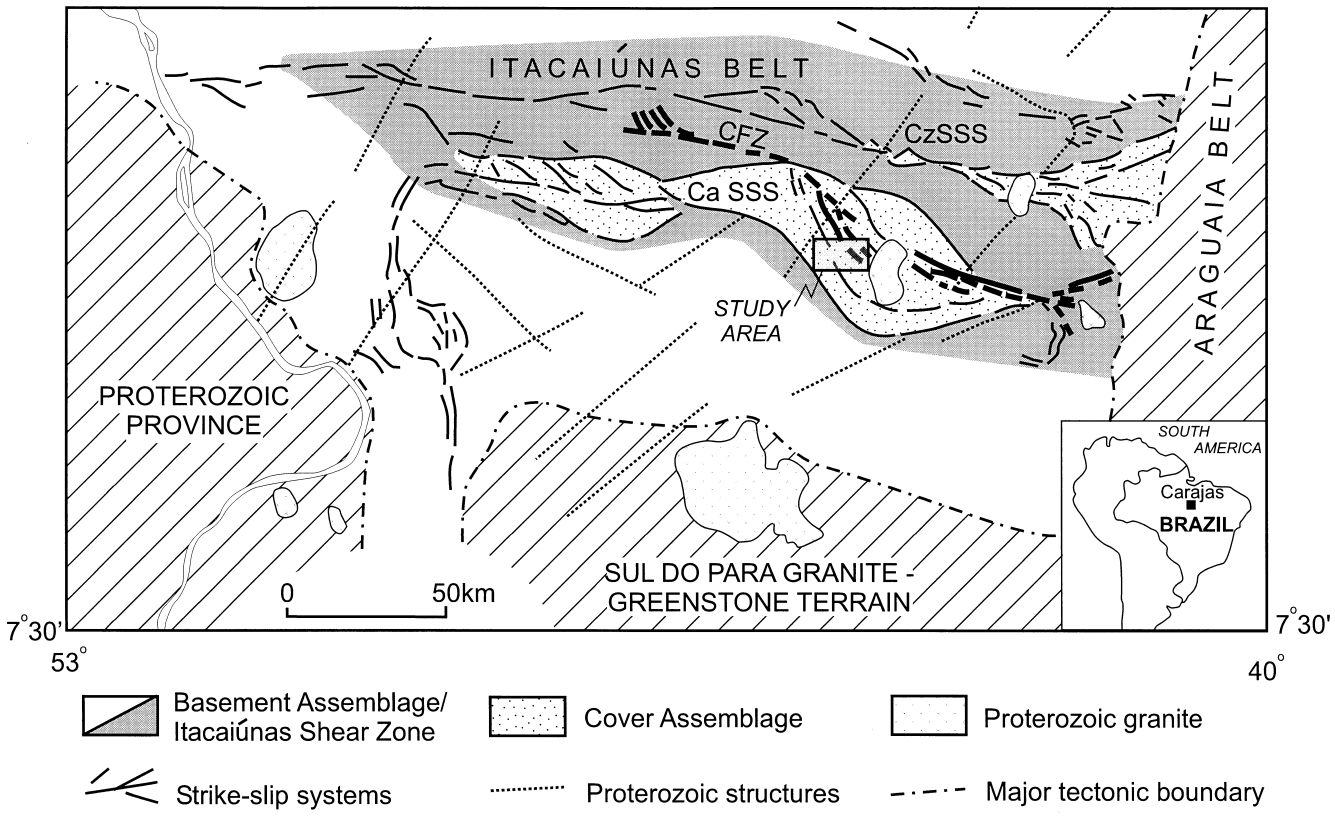


Fig. 1. Simplified regional structural map of the Itacaiúnas Belt of the Amazonian Craton, Brazil. The location of the Itacaiúnas Shear Zone in the basement rocks is indicated by shading. Late Archaean structures: CFZ—Carajás Fault Zone; CaSSS—Carajás strike-slip system; CzSSS—Cinzento strike-slip system. Box shows location of study area (Fig. 3a).

amphibolite facies orthogneisses and migmatites (Xingu Complex; ca. 2.85 Ga; Machado et al., 1991) and syn-tectonic granitoids (Plaquê Suite; Araújo and Maia, 1991). Collectively, these units are referred to as the Granite–Gneiss Complex (Fig. 2b and c; see also Silva et al., 1974; DOCEGEO, 1988; Pinheiro, 1997). In addition, there are isolated occurrences of high-grade supracrustal rocks of probable volcanic and sedimentary origin known as the Igarapé Salobo Group (ca. 2.85 Ga; DOCEGEO, 1988; Machado et al., 1991) associated with the western end of the CzSSS. All Basement Assemblage rocks are affected by

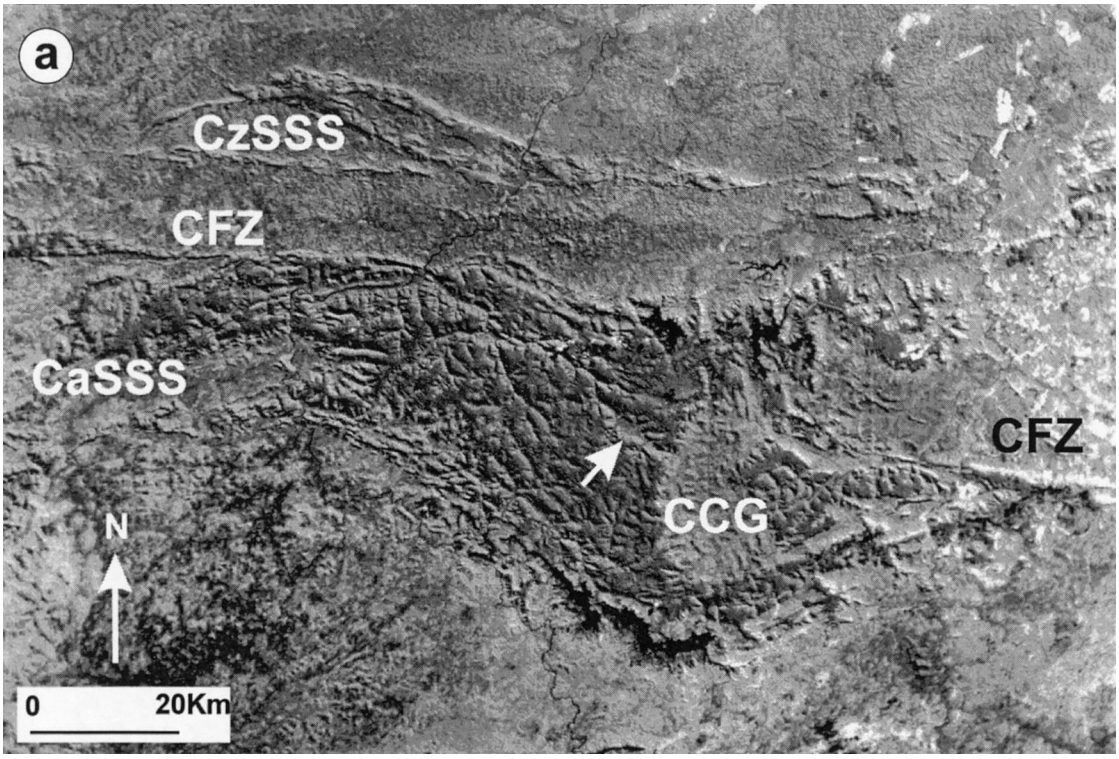


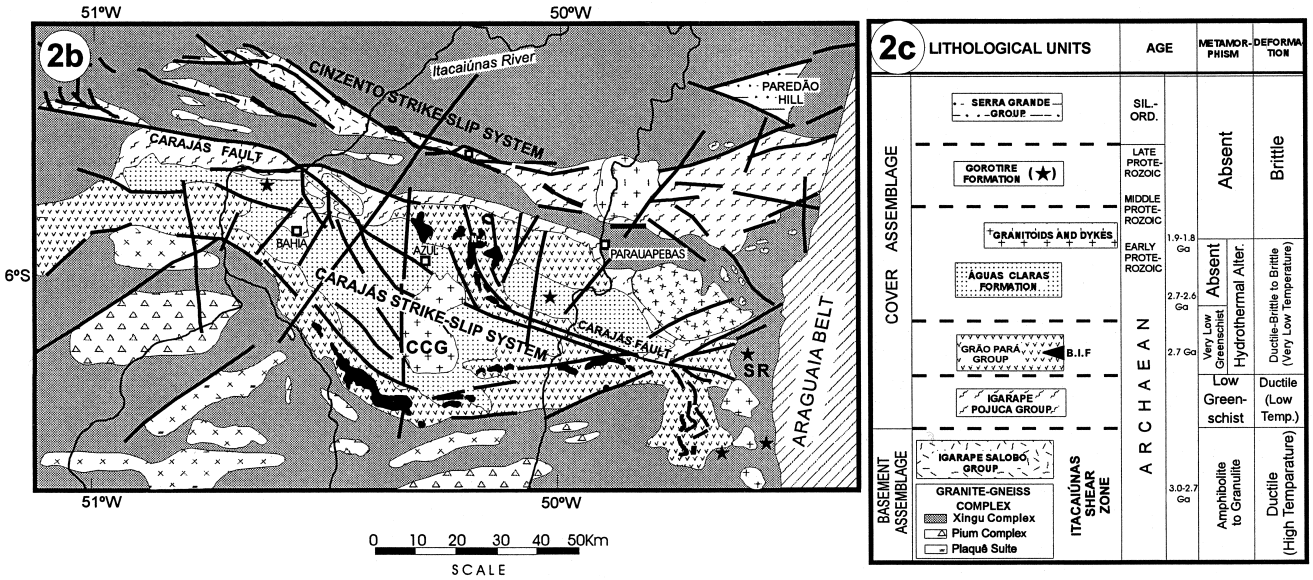


Fig. 2. (a) LANDSAT image of the Carajás region in the eastern part of the Itacaiúnas Belt. Key to abbreviations as in Fig. 1. Arrow points to location of Águas Claras River valley. (b) Simplified geological map of the Carajás region; '*' = Gorotire Formation outcrops. Key to lithologies in (c). CCG = Central Carajás Granite. SR = Serra do Rabo region. Based on DOCEGEO (1988), Araújo and Maia (1991), Siqueira (1990) and Pinheiro and Holdsworth (1997a). (c) Table summarising the tectonostratigraphy of the Carajás region. BIF = Banded ironstone formations.

ductile deformation and upper amphibolite facies metamorphism associated with the Late Archaean Itacaiúnas shear zone (Fig. 1; ca. 2.8 Ga; Machado et al., 1991), which forms a broad system of linked, moderately to steeply dipping sinistral strike-slip and thrust-dominated shear zones (Araújo and Maia, 1991).

The CaSSS and CzSSS post-date the Itacaiúnas shear zone and formed during later regional phases of brittle–ductile to brittle deformation that are mainly localised along the fault zone arrays. There is widespread field evidence, however, that the orientations of the faults were strongly controlled by the trend of pre-existing ductile fabrics in the underlying Basement Assemblage (Pinheiro and Holdsworth, 1997a). The steeply dipping fault systems exhibit the curved and braided patterns that are typical of strike-slip fault zones and preserve direct and indirect evidence for several phases of dextral and sinistral movement since ca. 2.8 Ga (Table 1; Pinheiro, 1997). The same faulting and associated folding events also affect overlying, low to very low metamorphic grade supracrustal volcanic and sedimentary rock sequences of Late Archaean age. These units form the older, dominant part of the *Cover Assemblage* (Fig. 2b and c; Pinheiro, 1997; Pinheiro and Holdsworth, 1997a,b). The cover rocks are either known or are inferred to rest unconformably on the Basement Assemblage. The lower part of the Cover Assemblage comprises a sequence of greenschist-facies clastic sedimentary rocks (Igarapé Pojuca group, DOCEGEO, 1988) unconformably overlain by very low grade volcanics and ironstones (Grão Pará group; ca. 2.76 Ga; Wirth et al., 1986; Machado et al., 1991) and younger, unmetamorphosed sequences of shallow-water marine to fluvial clastic deposits (Águas Claras formation; Nogueira et al., 1995) (Fig. 2c; see below). These rocks are intruded by weakly deformed ca. 1.8 Ga A-type granitic plutons and basic dykes (Wirth et al., 1986; Dall'Agnol et al., 1987; Machado et al., 1991) that were emplaced during a mid-Proterozoic phase of regional extension or dextral transtension (Costa et al., 1991; Pinheiro and Holdsworth, 1997a). The upper, volumetrically subordinate part of the Cover Assemblage comprises thin, localised sequences of presumably later Proterozoic immature clastic sedimentary rocks (Gorotire formation) and Phanerozoic sedimentary rocks (Sierra Grande group) (Fig. 2b and c). The rocks of the Gorotire formation are thought to post-date the 1.8 Ga plutons as they contain numerous clasts that are petrographically identical to these granitoids (Pinheiro, 1997). Minor fault reactivation episodes are likely to have occurred during the Phanerozoic and the location of recent small-scale earthquakes and hot springs along the major fault strands suggests that the region is still tectonically active (Costa et al., 1993; Pinheiro, 1997).

### 2.2. Relative timing and possible causes of basin development and inversion

On a regional scale, Cover Assemblage rocks are closely associated with the CaSSS and CZSSS fault strands and are preserved adjacent to bends, offsets and splays (Fig. 2b). This has led several authors to suggest that the cover rocks were laid down in a series of small dilational jogs or pull-apart basins during a phase of dextral strike-slip movements (e.g. Siqueira, 1990; Araújo and Maia, 1991). More recent sedimentological and structural studies (e.g. Nogueira et al.,

Table 1
Summary movement histories for the Carajás and Cinzento strike-slip systems

| Age (Ga) | Event | Kinematics |
|---|---|---|
| | Reactivation of fault systems recorded by recent small-scale seismicity | Uncertain |
| 0.24–0.15 | Reactivation of fault systems during opening of the South Atlantic in the Mesozoic. Development of small graben | Extension |
| | Deposition of the Serra Grande group during Siluro-Ordovician | Extension (intracratonic Parnaíba basin) |
| 1.9 | Intrusion of granite plutons and dyke swarms | Extension (or transtension) |
| | Weak tectonic inversion of the rocks by fault reactivation. Moderate to strong deformation of the rocks immediately adjacent to the Carajás fault | Sinistral transpression |
| 2.6 | Development of the Carajás and Cinzento strike-slip systems. Units were down-faulted inside major dilational jogs formed along the fault systems. Intrusions of sills and dykes. Formation of the Carajás fault | Dextral transtension |
| | Deposition of the Águas Claras formation | Large extensional (intracratonic) basin (geometry unknown) |
| 2.7 | Deposition, extrusion and intrusion of the Grão Pará group volcanics and ironstones. Later affected by low to very-low metamorphism (after 2.76 Ga) | |
| | Igarapé Pojuca group rocks affected by metamorphism and deformation at low to medium temperature conditions | Sinistral transpression |
| 2.8 | Itacaiúnas shear zone. High temperature ductile deformation affecting the Basement Assemblage | Sinistral transpression |

1995; Pinheiro and Holdsworth, 1996, 1997b) have shown, however, that a pull-apart basin model is inconsistent with the stratigraphic and facies patterns of the Grão Pará group and Águas Claras formation. All these rocks appear to have been deposited in sedimentary basins of regional dimensions prior to the onset of brittle strike-slip faulting. Dextral movements then faulted down previously deformed (Igarapé Pojuca group) and undeformed (Grão Pará group, Águas Claras Formation) cover rocks into the basement in a series of dilational jogs located along the major fault strands. It is difficult to ascribe individual structures in either basement or cover to this dextral event due to overprinting deformation during subsequent sinistral and dextral reactivations. It therefore remains a conjectural episode, based on the Z geometry of the curving fault systems and spatially associated, downfaulted units of Cover Assemblage rocks.

Regionally, the low-temperature deformation associated with the main phase of sinistral movements that affects the rocks of the Cover Assemblage is localised along major fault strands or adjacent to pre-existing fault jogs, bends and offsets. Major fault strands are exposed cutting basement rocks and older parts of the Cover Assemblage (Igarapé Pojuca and Grão Pará groups) at the SE end of the CaSSS, 50 km SE of Parauapebas (Serra do Rabo region; Fig. 2b). They comprise broad zones, tens of metres wide, of hydrated cataclasite, breccia and phyllonite that have undergone intense syn-tectonic to post-tectonic quartz veining and hydrothermal alteration. If these examples are typical of the region as a whole, the intensity of fluid-related alteration is likely to have caused long-term fault zone weakening that may account for the long history of regional fault reactivation (Holdsworth et al., 1997). However, the general paucity of exposed fault zones elsewhere in the basement rocks of the CaSSS and CzSSS means that this hypothesis remains speculative.

### 2.3. The Águas Claras formation and the CFZ

The Águas Claras formation crops out over an area of approximately 900 km$^2$ in the central part of the Carajás strike-slip system and is cross-cut in its central part by the Carajás fault zone (CFZ) (Fig. 2b). The largely unmetamorphosed sedimentary sequence is inferred to lie unconformably on the older, low-grade metamorphosed volcanic rocks of the Parauapebas formation and ironstones of the Carajás formation, both of which belong to the older Archaean Grão Pará group (Araújo and Maia, 1991; Pinheiro and Holdsworth, 1997b). The basal contacts of the Águas Claras formation are not exposed in the field.

The Águas Claras formation is composed of marine to fluvial sedimentary rocks, comprising up to 1500 m of mainly sandstones that are cross-cut by early gabbroic sills in the central part of the region. These intrusions yield an age of 2645 ± 12 Ma (Pb/Pb, zircon; Dias et al., 1996) that is thought to date intrusion, suggesting, therefore, that the Águas Claras formation is an Archaean age sequence. The sedimentary rocks and early basic sills are cross-cut and locally deformed by the CFZ. In this paper, we argue that the deformation of the Águas Claras formation occurred prior to the full lithification of the sedimentary rocks suggesting that the main phase of fault movement(s) was Late Archaean (ca. 2.6 Ga). The CFZ is cross-cut by the Central Carajás Granite (Fig. 2), a little-deformed pluton that was emplaced into the central part of the outcrop of the Águas Claras formation at 1880 ± 2 Ma based on a U/Pb zircon age obtained by Machado et al. (1988). Xenoliths of sedimentary rocks and a thermal aureole are preserved especially around the NE margin of the pluton (e.g. Wirth, 1986; Rios, 1991). Swarms of mafic dykes of uncertain radiometric age (?Middle Proterozoic) also cross-cut the sedimentary rocks and deformation structures related to the CFZ.

On satellite images of the region, lineaments corresponding to the CFZ cut NW–SE across the Águas Claras formation with a slightly NE-concave trace in map view (Figs. 1 and 2a). In detail, the fault appears to be a composite structure, comprising an approximately 1–2-km-wide zone of anastomosing lineaments that enclose rhomb-shaped units elongate in a NW–SE direction. Several branches diverge from the main fault trace forming a series of concave splays to the NE and SW (Fig. 2b; Pinheiro, 1997). Straight, relatively continuous NNE–SSW lineaments appear to cross-cut those trending NW–SE.

In the field, a 1–2-km-wide zone of metre- to tens of metre-scale folds and sinistral strike-slip faults is developed in the otherwise very weakly deformed sedimentary rocks of the Águas Claras formation adjacent to the main trace of the CFZ. These complex structures are best exposed in a series of roadcuts that transect the fault zone in the Águas Claras River valley (Figs. 1 and 3).

## 3. Stratigraphy and structure, Águas Claras River area

### 3.1. Stratigraphy

A transect through the main trace of the CFZ is exposed in a 7 km road section on the route joining the N-4 and Bahia mines in the valley of the Águas Claras River (Fig. 3). The NW–SE-trending CFZ cuts across a variety of sedimentary lithofacies (A–E) of the Águas Claras formation. These deposits are thought to form part of a tidal shoreface and fluvial to

deltaic braided system (Nogueira, 1995; Nogueira et al., 1995).

Sequence A is composed of mudstones and siltstones interpreted to be marine, or offshore platform deposits. The main primary structures preserved are climbing wave-rippled cross-lamination, parallel lamination, ripple marks, swaley cross-stratification and hummocky cross-bedding in storm sand sheets. Sequence B is at least 50 m thick and includes mainly fine to coarse sandstones with swaley cross-stratification, hummocky cross-bedding, symmetrical ripple marks and parallel lamination. These rocks are interpreted to represent storm-dominated platform deposits and they are faulted against sequence A to the NE by a NW–SE normal fault dipping at high angles towards the SW (Fig. 3). Sequence C is composed of sandstones and mudstone/siltstones with parallel lamination, load casts, symmetrical ripples and tabular cross-stratification. These rocks are interpreted to be braided, tide-dominated deltaic deposits. The rocks of the overlying

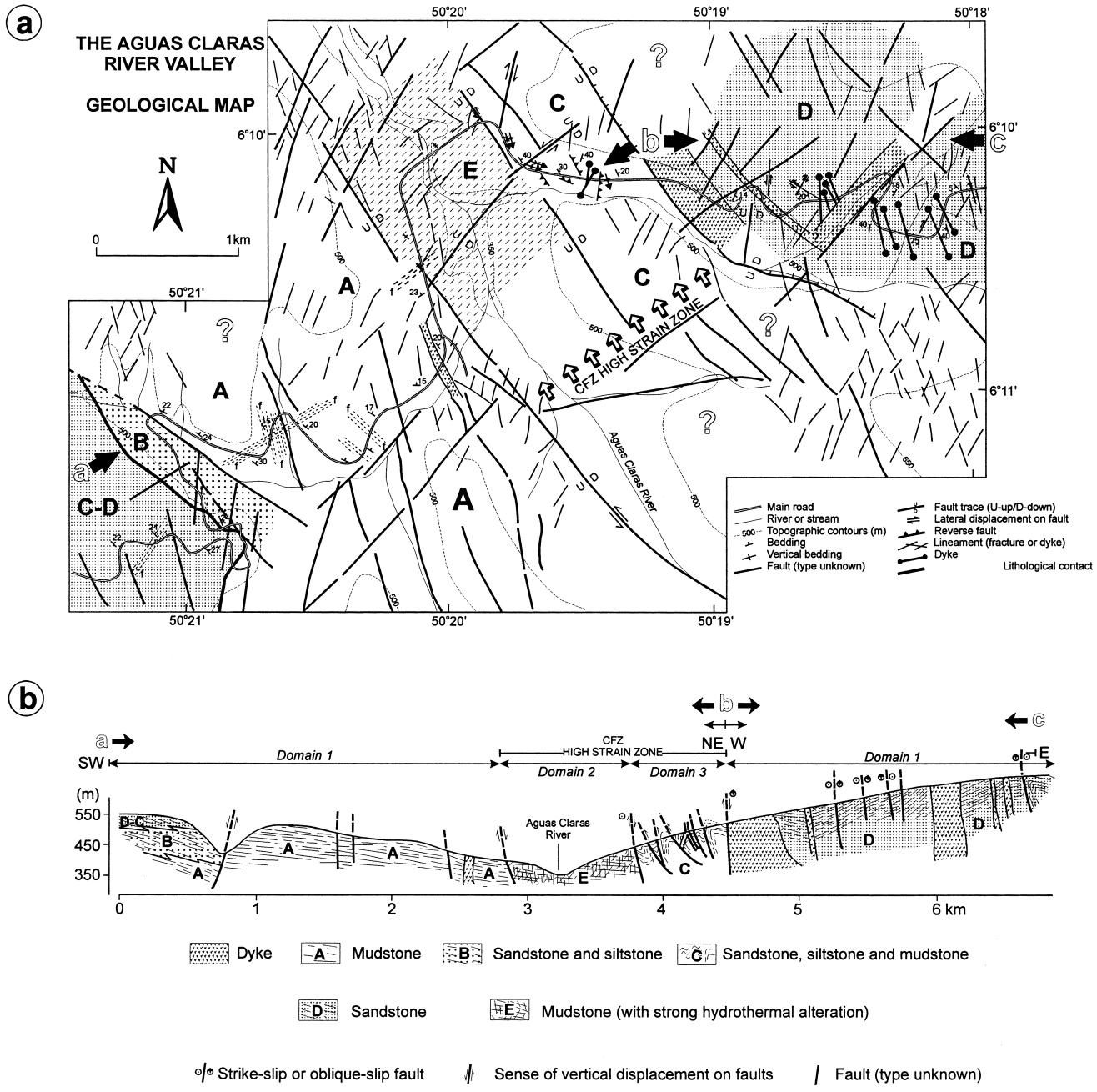


Fig. 3. (a) Geological map of the Águas Claras River valley showing distribution of lithofacies and structures. Location of cross-section in (b) also shown. (b) Cross-section through the CFZ and adjacent regions, Águas Claras River Valley area. Shows location of structural Domains 1–3.

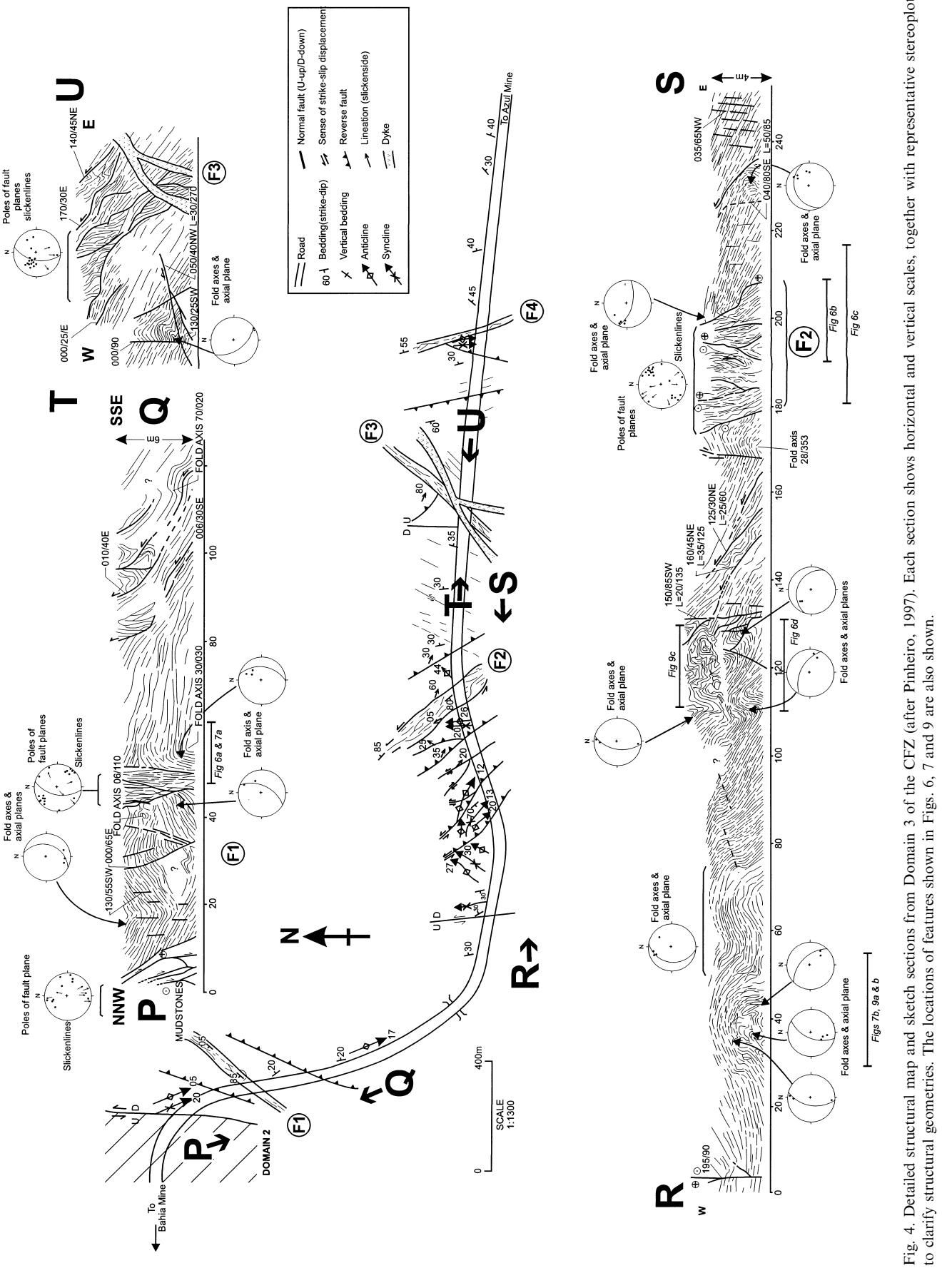


Fig. 4. Detailed structural map and sketch sections from Domain 3 of the CFZ (after Pinheiro, 1997). Each section shows horizontal and vertical scales, together with representative stereoplots to clarify structural geometries. The locations of features shown in Figs. 6, 7 and 9 are also shown.

sequence D are fine- to coarse-grained, braided sandstones and polymictic conglomerates with abundant tabular cross-stratification, trough cross-stratification and parallel lamination. These rocks are thought to be fluvial and deltaic deposits. The mudstone-dominated rocks of sequence A are assigned to the Lower Member of the Águas Claras formation whilst the stratigraphically overlying sequences (B–D) form the Upper Member (Nogueira 1995).

In the region of the Águas Claras River valley, the stratigraphic sequence is dismembered by a series of major faults that also define three domains (1–3) characterised by very different deformational structures (Figs. 3 and 4). Domain 1 represents the weakly deformed marginal regions of the CFZ, whilst Domains 2 and 3 form a central, more highly deformed fault core.

### 3.2. Structure of the CFZ

#### 3.2.1. Domain 1

Domain 1 corresponds to the 3 km and 2 km of section shown in Fig. 3(a) and (b) that lie on the SW and NE margins of the CFZ, respectively. It includes the mudstone-dominated rocks (sequence A) that are stratigraphically overlain by sandstones, siltstones and mudstones (sequences B–D), although the original stratigraphic contact is faulted out in this area (Fig. 3b).

Very few tectonic structures are present in the rocks of Domain 1. To the SW of the CFZ, the bedding shows a fairly constant NW–SE strike, dipping gently to the NE. On the NE margin, the bedding is more varied in orientation, striking mainly NNW–SSW to NE–SW and dipping 20–40° W to NW. In general, the beds show a significant component of dip in towards the core of the CFZ (Fig. 3b). Systematic fracture sets with a spacing of between 10 and 50 m occur throughout Domain 1 and some display normal and strike-slip fault movements that have caused localised tilting of the bedding. The orientation of these steeply dipping fracture sets is predominantly NE–SW, NNW–SSE and also N–S.

There are few folds in Domain 1, although a metre-scale monoclinal fold is associated with a sub-vertical, N–S fault located near to the NE end of the section (Fig. 3b). The fold plunges 30°N with a moderately to steeply NE dipping axial surface and is very similar in style to the folds seen in Domain 3.

A 300-m-thick dyke orientated NW–SE cuts sequence D rocks in region NE of the CFZ (Fig. 3a and b) together with several smaller dykes oriented mostly NNW–SSE and to a lesser extent NE–SW and NW–SE. Zones of pale-coloured hydrothermal alteration with thickness of about 5–15 m also occur subparallel to the dykes and are probably of a similar age. Most of these dykes are steeply dipping, tabular intrusions. They are also seen within the central part of the CFZ and on the SW margin where they display similar trends. Regionally, the thicker dykes (>100 m) trend NW–SE and NE–SW and correspond to prominent lineaments seen on satellite images with a typical spacing of 1–2 km (Pinheiro, 1997).

#### 3.2.2. Domain 2

Domain 2 forms an approximately 1-km-wide zone of cataclastic, altered rocks (labelled E in Fig. 3a and b) running nearly parallel to the NW–SE Águas Claras River valley. It is bounded by major NW–SE normal–oblique (sinistral) faults corresponding to important regional lineaments observed in satellite images. Few exposures occur in this zone of low-lying, flat topography. The rocks are greatly altered by hydrothermal and weathering processes, with the main rock type being fractured, red–green to white coloured mudstones or siltstones that are similar in appearance to those of Sequence A. A weak lamination is preserved in less sheared regions, but it is not possible to demonstrate that this is bedding.

Closely spaced fractures are widespread, trending NW–SE and defining a strong disjunctive anastomosing foliation—or 'fracture cleavage'—of tectonic origin. Some fracture planes preserve slickensides, striations and slickenfibres showing quite variable plunge angles towards both the NW and the SE. In places, a very fine cleavage is developed in the mudstones orientated sub-parallel to the main fault planes, giving them a phyllonitic appearance. Intense shearing has also led to the local development of incohesive cataclastic breccias with fragments that vary in size from 5–10 cm to millimetres across. Quartz and other secondary phyllosilicate minerals form the matrix in these rocks (10–20%). Most rocks in Domain 2 have suffered intense silicification and kaolinitization due to hydrothermal alteration.

#### 3.2.3. Domain 3

Domain 3 corresponds to an 800-m-wide, NW–SE orientated block of rocks located in the central area of the region that is bounded by high-angle faults (Fig. 3). The rocks belong to sequence C comprising fine- to coarse-grained sandstones, conglomerates, siltstones and mudstones, and form part of the Upper Member of the Águas Claras formation as defined by Nogueira et al. (1995) and Nogueira (1995). The SW contact with the highly sheared rocks of Domain 2 is an oblique-slip fault zone with a predominantly sinistral movement component and a secondary normal displacement (Fig. 4). The fault zone comprises a linked array of N–S to NNW–SSE-striking, imbricate faults dipping steeply E. The NE boundary of domain 3 is

defined by the steeply dipping, normal faulted margin of a NW–SE dyke (Fig. 3a, b).

The structure of Domain 3 is significantly more complex than adjacent areas due to the presence of cm- to tens of metre-scale, complex fold and fault systems (Fig. 4). As a result, bedding is locally very variable in orientation, but it generally strikes NNW–SSE sub-parallel to or slightly clockwise of the main trace of the CFZ (Figs. 3 and 4). Bedding dips are mainly shallow to moderate and to the ENE, although the layering commonly steepens into subvertical orientations adjacent to larger faults. A single, heavily weathered, bifurcating dyke, striking NE–SW cross-cuts faults and associated folds in the road section zone (Fig. 4; section T–U). The structures from Domain 3 will now be described in more detail.

### 3.3. Detailed structure of the central CFZ

Most faults in Domain 3 are oblique-slip faults orientated NW–SW, N–S and NE–SW (Fig. 5a). The oblique-slip faults display both normal and reverse components, although the latter dominate, together with consistent sinistral displacements of different magnitudes. On a large scale, Domain 3 is cut by at least four major fault zones (labelled $F_1$–$F_4$, Fig. 4).

The folds in Domain 3 reflect a complex, heterogeneous strain pattern that is spatially linked to the development of contemporaneous fault systems (Figs. 4–9). Fold styles vary from Class 1B- to 1C-type structures with rounded hinges through to more kink-like or chevron fold shapes in profile. The folds are generally asymmetric and display mainly west to southwest

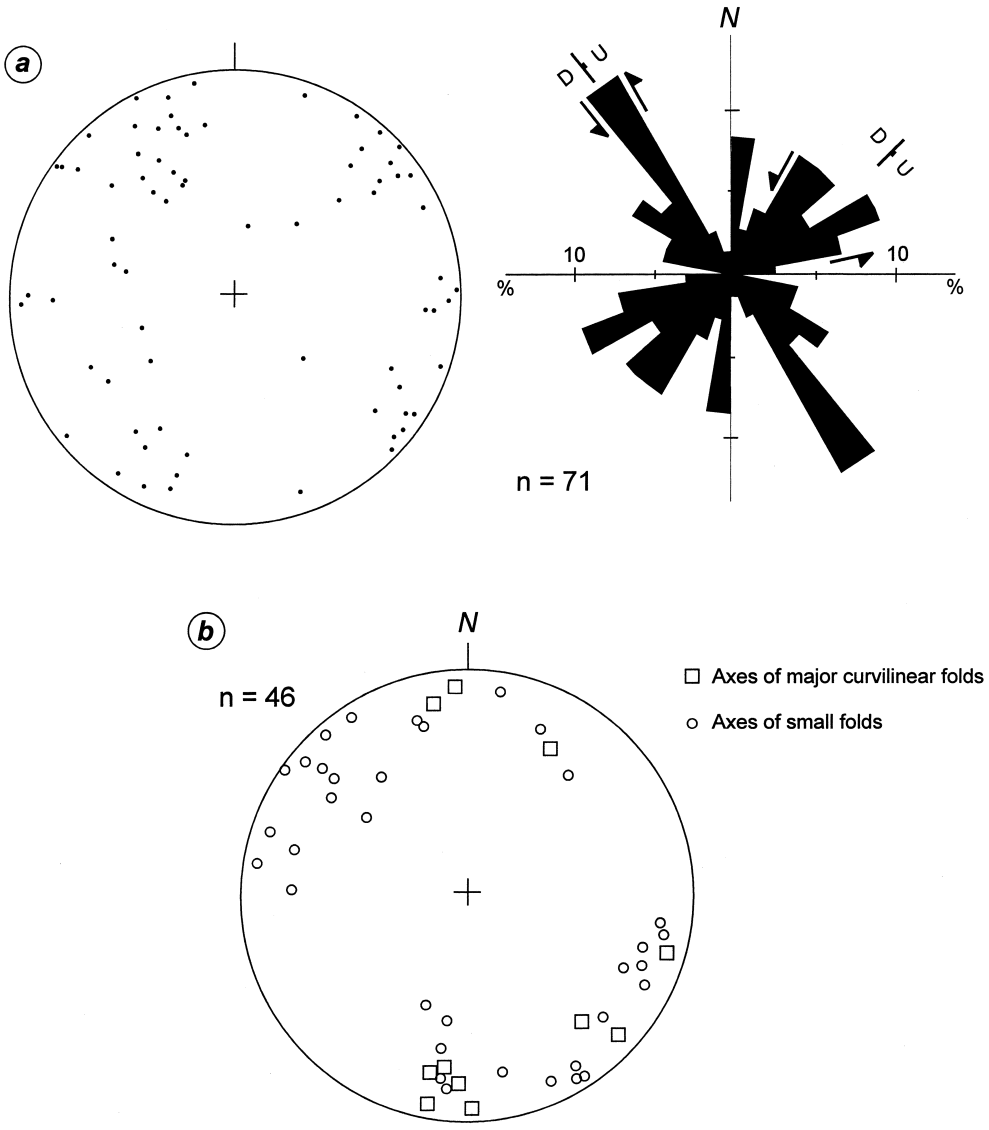


Fig. 5. (a) Stereoplot showing poles to fault planes and rose diagram showing fracture trends and senses of movement, Domain 3 of the CFZ. (b) Stereoplot of all major and minor fold axes, Domain 3 of the CFZ.

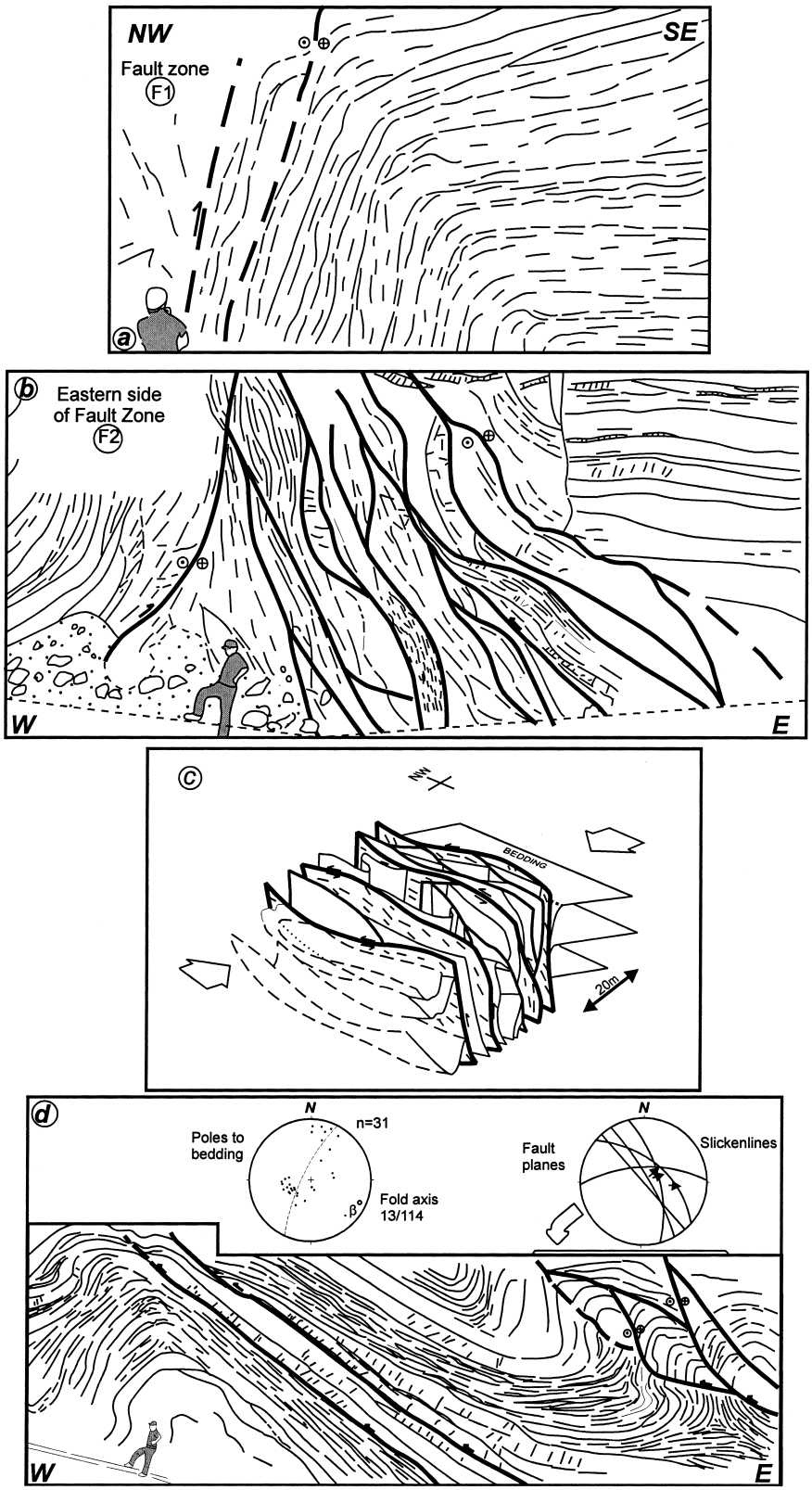


Fig. 6. Fold-fault associations from Domain 3 of the CFZ (all sketched from field photographs). (a) Monoclinal fold closure and faults on SE side of fault zone $F_1$—see Fig. 7(a) for original photograph. Compare geometry with fig. 7b of Sylvester and Smith (1976). (b) Interlinked network of sinistral oblique- and strike-slip faults on the east side of fault zone $F_2$—note that the oblique view shown here obscures the tight antiformal hinge immediately east of the fault zone (seen on Fig. 4). (c) 3-D diagram summarising the geometry of the monoclinal fold and fault zones, e.g. $F_2$. (d) Asymmetric folds and sinistral oblique thrusts. Locations of all views shown on Fig. 4.

vergence. Interlimb angles vary from gentle to very tight, often for individual structures over a distance of a few tens of centimetres. On average, folds trend subparallel to the trace of the CFZ, but in detail, many hinges are curvilinear through a few tens of degrees. More extreme angles of curvature (50–100°) occur locally on a centimetre scale producing complex and irregular closed outcrop patterns (Figs. 4, 7b and 9). Fold plunges are generally shallow (< 30°) with azimuths in the northwestern and southeastern quadrants, although the majority of metre- to tens-of-metre-scale folds plunge shallowly S, N or SE (Fig. 5b). Overall, fold axial planes are very variable in orientation, striking NW–SE, N–S and NE–SW, with mainly steep dips in various directions (Fig. 4). An occasional, very weak axial planar slaty cleavage is developed in mudstone units within some fold hinge zones; in other lithologies, tectonic fabrics are absent.

Three fold groups are recognised based on their geometry and relationship to adjacent faults. Based on field relationships, all these structures appear to be broadly contemporaneous and it is not always possible to assign individual folds to particular groups in every case. Nevertheless, we feel that the subdivision is useful and that it may provide an insight into differing mechanisms of fold formation. Each fold group is now described with reference to examples exposed in the road section.

*Monoclinal fold zones* are directly associated with major, steeply dipping fault zones ($F_1$, $F_2$ and $F_4$) striking NE–SW or NW–SE (Figs. 4, 6a,b and 7a). The fault zones are between 5 and 25 m across and coincide with the steep limbs of shallowly plunging (< 25°) monoclines that trend at low- to moderate-angles, or sub-parallel to the fault zone (e.g. the folds associated with fault zones $F_1$ and $F_2$, Fig. 4). The hinge regions of the monoclines may be partially or totally cut out by the faults. The vertical limbs of the

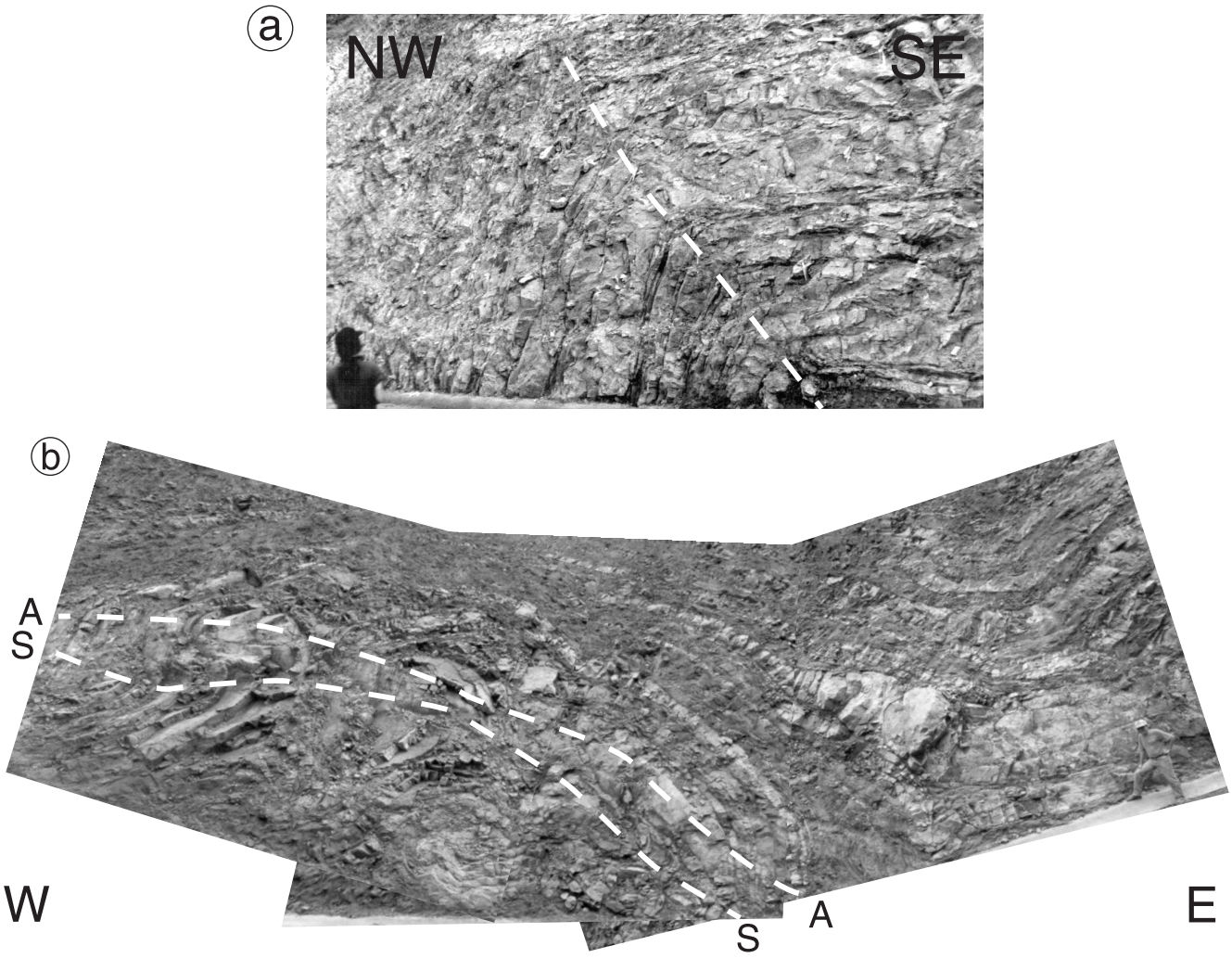


Fig. 7. (a) Field photograph of monoclinal fold closure and faults shown in Fig. 6(a). Dashed line indicates location of fold axial trace. (b) Field photograph of curvilinear polyclinal folds shown in Fig. 9(a). A and S correspond to antiformal and synformal axial traces shown in Fig. 9(a).

folds are cut by interlinked arrays of faults parallel to bedding planes or cross-cutting at low angles to produce imbricate zones (e.g. Fig. 6b and c). Slickenlines along fault planes plunge mostly at low angles (10–20°), but steeper orientations are also present (see small stereonets in Fig. 4). The sense of shear along many individual faults is not easily deduced in the field since kinematic indicators are only sporadically preserved. Slickenfibres are developed on some fault planes and more than one set may be present on a single fault plane suggesting a complex movement history. Other slip-sense indicators observed include slickenline steps and secondary T-fractures arrays that are seen in plan view along some faults. Collectively, these structures suggest a predominance of oblique-sinistral faults with a subordinate high-angle reverse displacement, i.e. generally E-side up—note that this agrees with the sense of apparent top-to-the-west vergence of the monoclines (Fig. 4).

In the steeply dipping fault zones coinciding with monocline common limbs, small open to close folds of bedding occur locally between fault strands, especially where sandstones are interbedded with mudstones (Fig. 6c). The orientation of these irregular folds can be rather variable—some plunge at low angles forming isolated synclines or anticlines, whilst others plunge steeply to sub-vertically forming neutral folds. There is no systematic pattern to this minor folding.

Isolated examples of monoclinal folds and associated steeply dipping faults occur locally in other domains in the Águas Claras River valley, notably at the eastern end of the road section in Domain 1 (Fig. 3b).

*Asymmetric folds and oblique thrusts* are mainly metre- to centimetre-scale features that are commonly associated with moderately to shallowly NE- to SE-dipping faults in the section. Three prominent thrust belts are developed in the road section (Fig. 4): at the south end of section P–Q; 110–165 m from the eastern end of section R–S; and forming the prominent SE-dipping fault zone (F3) in section T–U.

The majority of folds plunge NW–SE and have steeply dipping axial planes striking NW–SE or N–S (Fig. 4). Most folds verge westwards, although several metre-scale structures verge eastwards and are characterised by flat-lying or westerly dipping axial surfaces (e.g. 10 m west on section T–U; 230 m west on section R–S; Fig. 4). The NE- and SE-dipping faults associated with these folds preserve slickenlines indicating predominantly sinistral reverse displacements (Figs. 4, 5a and 6d). A subordinate group of faults, dipping 40–80° NE or E show predominantly reverse displace-

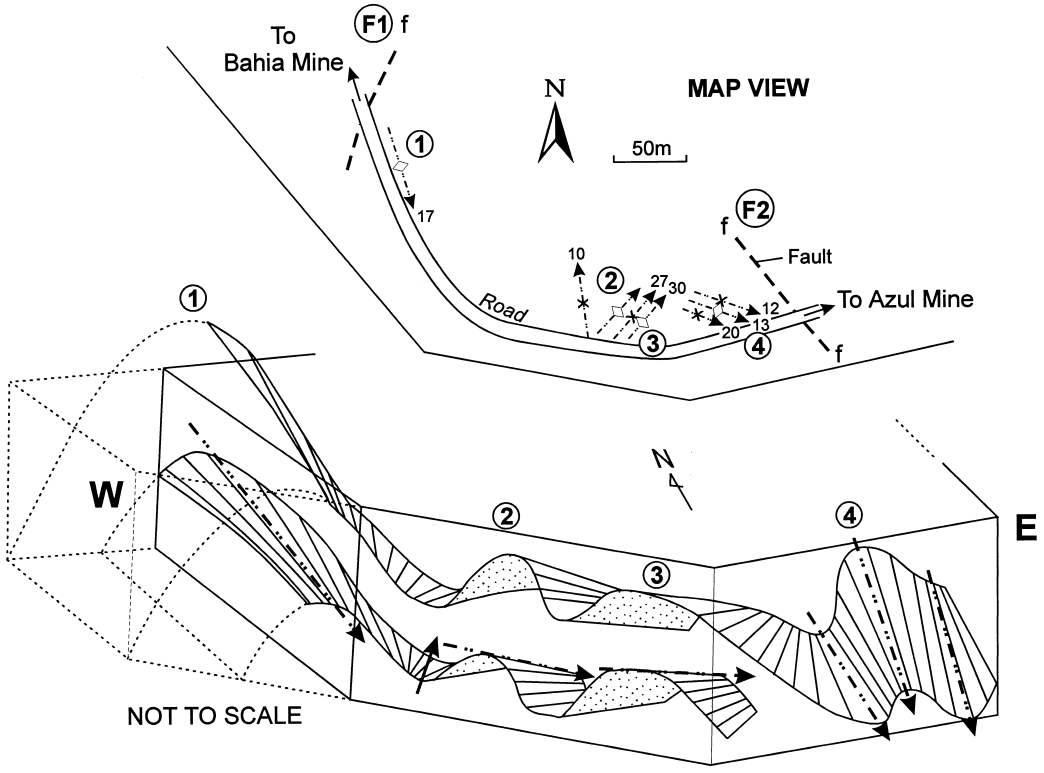


Fig. 8. Map and 3-D diagram of complex folds from SE-side of Domain 3 of the CFZ. Numbers refer to anticlines mentioned in the text. Note positions of fault zones $F_1$ and $F_2$ for reference.

ments and are typically sub-parallel to bedding (Fig. 6d).

*Polyclinal, complex folds* occur as a number of metre- to tens of metre-scale anticlines and synclines that are characterised on all scales by variable plunges, curvilinear hinges and curviplanar, locally polyclinal axial surfaces (e.g. anticlines 1–3, Fig. 8). Unlike the other two groups of folds, they are not generally associated with faults. The folds are mostly open to close with rounded to box-fold profile shapes. The most complex part of these structures occurs in the inner hinge regions of some folds. The best exposed example occurs in the core of the anticline about 40 m from the beginning of the R–S section (Figs. 4, 7b and 9a; anticline 2 in Fig. 8). Another, less well-exposed example occurs in the upper part of the roadcut about 120 m along the same section (Fig. 4; above anticline 4 in Fig. 8). In both cases, these regions are characterised by the development of complex and irregular closed outcrop patterns.

In the first example, a series of highly curvilinear, disharmonic folds are developed plunging shallowly SSW, SE and NW in the core of a large anticlinal composite box fold (Figs. 7b and 9a). The pattern of folds appears to be a highly localised dome-and-basin conical fold or interference pattern with two curvilinear fold hinge directions discernible plunging NW or SE (K and L) and variably SSW (M) (Figs. 7b, 9a and b). The contours of poles to bedding (Fig. 9b) suggest a conical structure with an axis plunging 55° towards 335°. It is also possible, however, to define three β-axes corresponding approximately to the fold axes K, L and M observed in the field. Minor fold axes measured in the field are also shown for comparison (Fig. 9b). The second example exposed further to the east in the upper part of the road cut displays a very similar and somewhat tighter conical geometry (Figs. 4 and 9c). These folds presently lie adjacent to a prominent zone of SW-verging asymmetric folds and oblique thrusts, including a prominent set of folds in the lower part of the roadcut (see Figs. 4 and 6d; includes the anticline 4 in Fig. 8). The relationships between these structures are unclear due to a zone

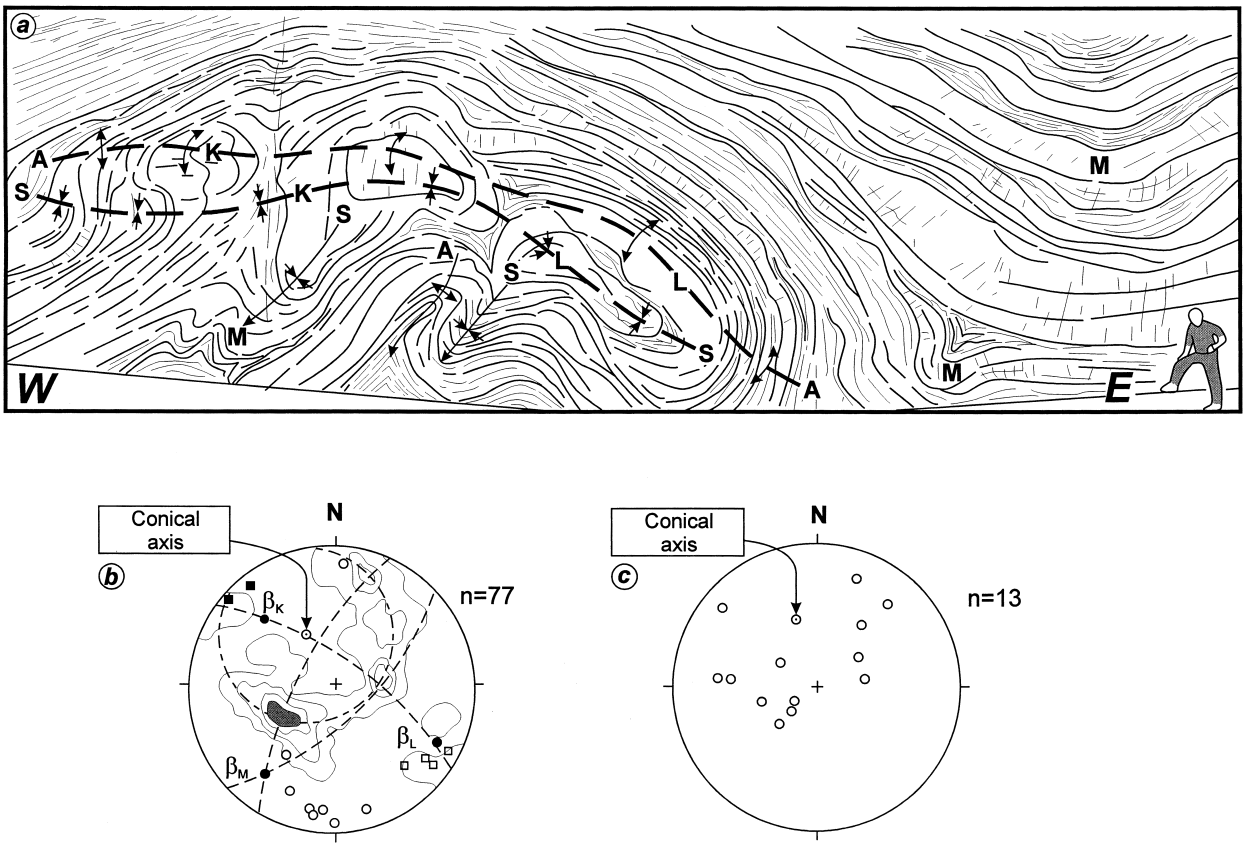


Fig. 9. Complex curvilinear and polyclinal folds from Domain 3 of the CFZ—locations shown on Fig. 4. (a) Field sketch (from photograph in Fig. 7b) of complex folds 40 m from west end of section R–S in Fig. 4. Key: A = antiformal axial trace; S = synformal axial trace; K, L and M = fold sets referred to in text and shown in (b). (b) Stereoplot of poles to bedding ($n$ = 77) around folds shown in (a) and measured minor fold axes (K = closed boxes; L = open boxes; M = open circles). Best-fit conical fold axis to foliation data shown, together with three profile planes and axes that approximately match orientation of fold sets K, L and M. (c) Stereoplot of minor fold axes and best-fit conical fold axis from complex folds in upper part of section 120 m from the western end of the R–S section (for location, see Fig. 4).

of poor outcrop separating the two levels of the roadcut (blank area on Fig. 4)—the break in exposure may indicate the presence of a fault.

The thickness of beds involved in these curvilinear folds is variable. Sandstones show a tendency to be thinned towards hinge regions whilst mudstones thicken to develop bulbous hinge zones. Millimetre-scale tensile quartz veins are present only locally, forming en-échelon sets particularly in the folded sandstones.

*Normal faults* are subordinate features in Domain 3 and usually show a small component of strike-slip displacement. They are predominantly N–S-striking, steeply dipping features, with small (<3 m) E-side-down displacements in most cases. An example occurs at the extreme western end of the R–S section (Fig. 4). Subvertical, NW–SE normal faults delimit the present day margins of Domain 3, exhibiting a minimum throw of 200 m based on the measured offsets of the stratigraphic sequences (Fig. 3b; Pinheiro, 1997). The normal faults are all thought to form mainly during later regional episodes since small-scale normal faults consistently cross-cut all folds and oblique-slip faults. Those delimiting Domain 3 are, therefore, presumed to reactivate pre-existing sinistral structures.

## 4. Discussion

### 4.1. Large-scale structure of the Águas Claras River valley

The Carajás strike-slip system is dominated by the formation of faulted blocks on a kilometre-scale (Pinheiro, 1997) and this is illustrated well by the large-scale geometry of the CFZ in the Águas Claras River valley (Fig. 10a). NW–SE elongated rhomb-shaped fault blocks are defined by sets of steeply dipping faults orientated NW–SE and NE–SW, with a variable spacing of approximately 1–2 km (Figs. 3a and 10a). Many of these faults form marked lineaments observed with these trends in satellite and radar images (Fig. 2a). At this scale, there is a predominance of normal and oblique–sinistral strike-slip displacements, with vertical offsets in the order of a few hundred metres or less based on the observed offsets in the stratigraphy.

The intensity and style of deformation within the fault-bounded blocks varies markedly. Those forming Domain 1 (Figs. 3 and 10) are generally little deformed with only minor fracturing, block rotation and/or tilting. The elongate, poorly exposed block defining Domain 2 comprises highly sheared, hydrothermally

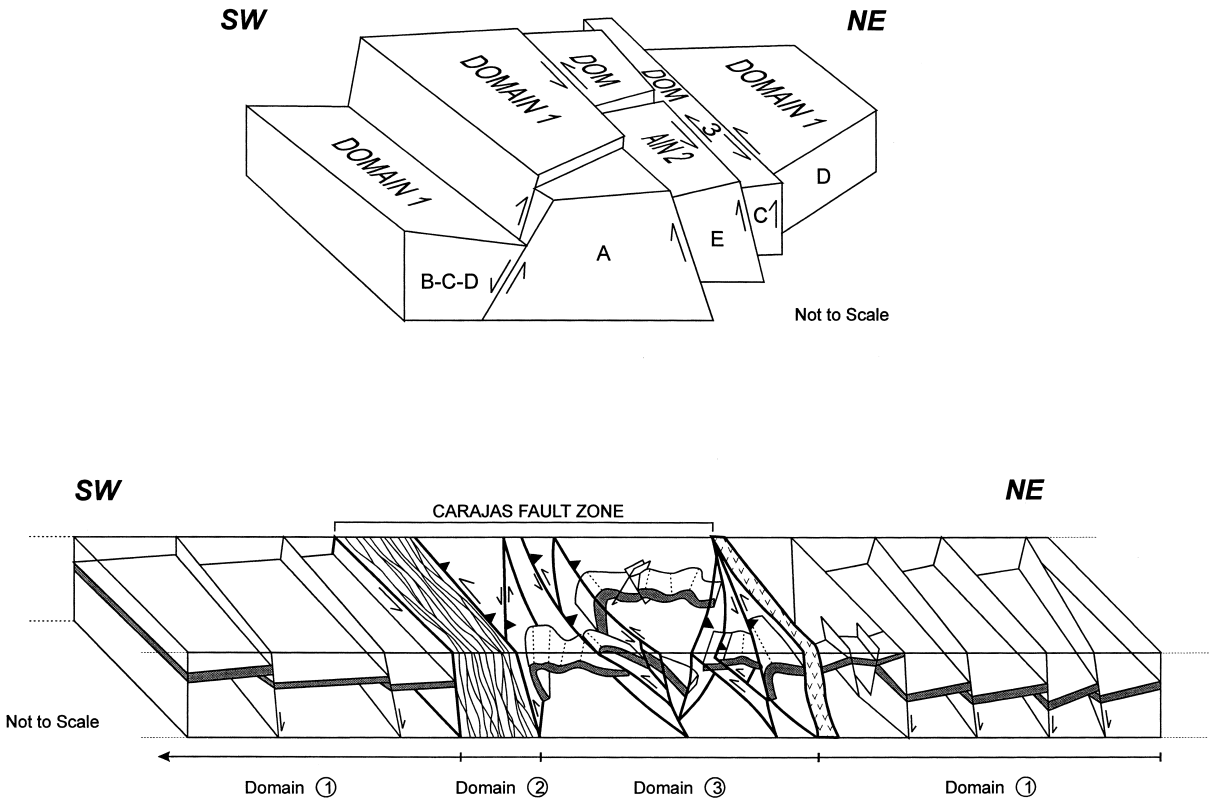


Fig. 10. Highly simplified 3-D sketch showing the orientation and relative vertical displacement of fault blocks in the Águas Claras River valley area (refer to Fig. 3a for location). (b) 3-D sketch summarising the general geometric and kinematic characteristics of structures in the CFZ of the Águas Claras River valley based on the findings of the present study. The structure of Domain 3 is interpreted to represent an asymmetric flower structure.

altered and strongly weathered rocks. It is thought to correspond to a major fault zone or to a highly fractured zone into which there has been a massive influx of hydrothermal fluids at a late stage in the tectonic history, possibly synchronous with the intrusion of the Central Carajás Granite ca. 1.8 Ga. Very poor exposure makes it difficult to discuss the deformation structures in this domain. Domain 3 preserves a remarkable and complex assemblage of meso-scale folds and closely associated faults that contrast strongly with the structural simplicity of the adjacent blocks (Fig. 10b). These features lie within the main set of lineaments that define the CFZ and are thought to record deformation associated with the main phase of sinistral transpression along this structure. The strain is highly localised forming an elongate belt ca. 1 km wide adjacent to the main fault in the rocks of the Águas Claras formation. In older, underlying rocks of the Grão Pará group, the effects of the same deformation event are distributed across broader regions several kilometres across (e.g. see Pinheiro and Holdsworth, 1997b; Pinheiro, 1997).

### 4.2. The formation of the folds and faults within the CFZ

There is no field evidence to suggest that the majority of folds and associated faults observed in Domain 3 formed during different regional events as they display geometric and kinematic characteristics consistent with a single phase of sinistral transpression. In particular, the repeated location of steeply dipping, oblique reverse-sinistral fault zones in the sub-vertical limb regions of large monoclinal folds suggests an intimate relationship between the development of folds and faults (Fig. 11a–d). It is suggested that high-angle, mainly reverse faulting in the basement localises the development of sub-parallel, monoclinal forced-folds (sensu Stearns, 1978) in the cover rocks of the Águas Claras formation (Fig. 11a). The orientation and vergence of the folds is essentially controlled at this stage

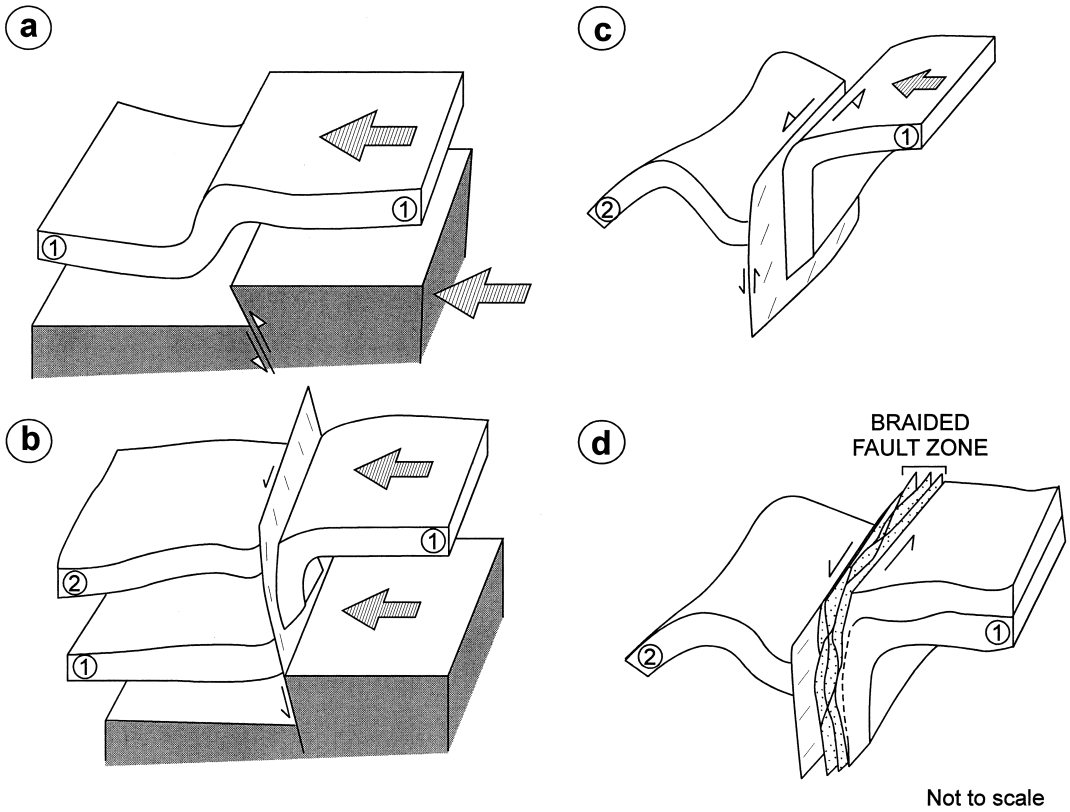


Fig. 11. Schematic diagrams to explain the evolution of the monoclinal fold/sinistral fault association observed in the Águas Claras River valley section of the CFZ. (a) Dominantly contractional offset along pre-existing fault zone in basement produces early forced, monoclinal folds in Águas Claras formation cover sequence. (b–d) Fault propagates up into steep common limb of folds and, as continued deformation tightens folds and rotates local bedding into sub-parallelism with fault, this region becomes increasingly favourably oriented for the accommodation of sinistral strike-slip displacements. In the diagram sequence, the effects of contraction and sinistral strike-slip are shown to locally decrease and increase, respectively, in response to the changing orientation of bedding anisotropy in the cover sequence. Note that spatial and temporal partitioning processes on this scale could occur at different times in different parts of the CFZ on a regional scale. The basement is not shown in (c) or (d). Layers 1 and 2 are labelled for reference.

by the vertical component (E-side-up) of fault movement. As the folds amplify, the basement fault propagates up into the common limb and a zone of steeply dipping to subvertical bedding develops that increasingly acts as an appropriately oriented locus for sinistral displacements, possibly leading to local spatial and temporal partitioning of contractional and strike-slip strains (Fig. 11b–d). Strain hardening could then lead to fault zone widening and imbrication in the steep fold limbs (Fig. 11d). Note that not all monoclinal folds have to reach the final stage of this evolutionary sequence.

The spatial association of steep sinistral reverse fault zones and more shallowly dipping, sinistral oblique- to dip-slip thrusts and mainly westerly verging folds (Fig. 10b) strongly suggests an asymmetric flower structure geometry. Unfortunately, there is insufficient vertical relief to observe the relationship between the steep fault zones and the thrusts, so this remains a matter of conjecture. The marked local variations in movement directions, even along individual faults suggest that complex small-scale partitioning of contractional and strike-slip strain components may have continuously changed in space and time (e.g. Laney and Gates, 1996).

Complex curvilinear folds are observed on various scales, some of which display dome-and-basin, conical forms. A sheath fold origin seems unlikely as such structures are generally associated with highly deformed belts of pervasive ductile deformation (e.g. Carreras et al., 1977; Alsop and Holdsworth, 1999). Therefore, three other possible models may explain the development of these curvilinear structures:

1. They are the products of locally constrictional strains ($1 < k \leq \infty$; cf. Flinn, 1962). This is thought to be unlikely because most transpression zones are characterised by flattening strains ($1 > k \geq 0$; Sanderson and Marchini, 1984). Constrictional strains in a transpression zone would require additional components of both lateral stretching parallel to the strike of the fault zone and sub-vertical shortening (e.g. Dewey et al., 1998) for which there is no independent field evidence.
2. They have formed due to a markedly non-parallel, 3-D oblique relationship between the bedding and the principal axes of finite strain leading to the simultaneous development of two sets of orthogonal fold axes (cf. Treagus and Treagus, 1981). This is possible if the bedding in some fault-bounded units was rotated into an oblique orientation prior to nucleation of folds. It is difficult to prove or disprove this model.
3. They are highly localised Type I interference patterns of Ramsay (1967) formed due to temporal strain partitioning in which one set of folds formed during contraction-dominated strain (e.g. fold sets K and L in Fig. 9) whilst the other set (e.g. set M in Fig. 9) formed during a phase of sinistral strike-slip- (or wrench-) dominated deformation. This model is consistent with the observed evidence of strain partitioning recorded by variations in the fault displacement directions.

We are unable to conclusively prove or disprove models (b) and (c) and it is possible that both models may be appropriate for different structures observed in the section studied. The lack of a well-defined, steeply dipping planar bedding anisotropy in the areas of highly curvilinear folds may account for the absence of associated fault structures.

The structures of the CFZ in the Águas Claras River valley differ significantly from the larger kilometre-scale folds and faults that formed during sinistral transpression affecting older units of the Cover Assemblage (Grão Pará group) associated with the nearby N-4 Ironstone deposit (Fig. 2b; see Pinheiro and Holdsworth, 1997b). This could reflect differences in the rheological behaviour of the different rock units involved, or may arise because the structures developed in the ironstones appear to be associated with transpressional deformation in a kilometre-scale restraining bend of the CFZ.

### 4.3. The timing of sinistral transpression along the CFZ

The clastic sequences of the Águas Claras formation form a tectonically preserved remnant of a wider and larger sedimentary basin (ca. 2.65 Ga) that were downfaulted into a dilational jog during an early phase of dextral displacement along the CaSSS (Pinheiro and Holdsworth, 1997a). This system was then subsequently inverted due to a later phase of sinistral displacement producing the transpressional structures described in this paper and elsewhere (e.g. Pinheiro and Holdsworth, 1996, 1997a, b; Pinheiro, 1997). These events are then post-dated by the intrusion of Middle Proterozoic plutons (ca.1.8 Ga), including the Central Carajás granite which cross-cuts the CFZ, possibly during a regional episode of extension or dextral transtension (Pinheiro and Holdsworth, 1997a).

The rocks of the Águas Claras formation are essentially unmetamorphosed and the deformation features associated with the CFZ therefore formed at relatively shallow crustal depths ($< 5$ km). Whilst the structure described here are of tectonic origin, certain features suggest that the rocks may not have been fully lithified at the time of deformation. These features include:

1. There is little evidence of low-temperature intracrystalline deformation synchronous with folding in the sandstones when they are examined in thin section. They appear homogeneous and undeformed and

lack internal deformation fabrics, features that are consistent with deformation dominated by frictional grain-boundary sliding during deformation (Maltman, 1984).
2. The locally complex and seemingly chaotic nature of some of the folds is reminiscent of structures formed during deformation of partially lithified rocks (e.g. Hobbs et al., 1976; Maltman, 1994). This might also explain the observed changes in thickness of the sandstones around many of the folds (cf. Elliott and Williams, 1988).
3. A partially lithified state would also be consistent with the highly localised nature of the deformation in these rocks where the deformation is largely driven by motions of fault blocks in the fully lithified rocks in underlying Basement and Cover Assemblage sequences.

If our proposal that the rocks of the Águas Claras formation were deformed prior to full lithification is correct, this implies that the sinistral transpressional deformation affecting these rocks is a late Archaean event (ca. 2.65 Ga).

### 4.4. Comparison with more recent structures

Most descriptions of the geometry and evolution of transpressional structures formed in shallow crustal environments are based on field studies or interpretation of seismic reflection profiles of deformed Mesozoic and Cenozoic strata (e.g. Wilcox et al., 1973; Sylvester and Smith, 1976; Dooley and McClay, 1996; Curtis, 1999). There are significant similarities between these later Phanerozoic structures and the Archaean-age features related to the CFZ in the Águas Claras River valley. Thus, the association between folds generally trending sub-parallel to the main strike-slip fault zone ('in-line' structures) and the linked systems of sub-vertical, sinistral faults and top-to-the SW thrusts (Fig. 10b) closely resembles the flower structures described by Wilcox et al. (1973) and Harding (1974) from various locations. The monoclinal fold-fault association described here (e.g. Figs. 4 and 6a–c) is strikingly similar to features formed during Cenozoic transpression along the Painted Canyon fault in the San Andreas fault zone (Sylvester and Smith, 1976, e.g. compare their fig. 7b with Figs. 6a and 7a). Conversely, the complex mesoscale folding patterns observed in the Águas Claras road section point to a hitherto unrecognised structural complexity that may exist adjacent to fault zones in many Cenozoic and Mesozoic settings. Most published accounts refer only to structures developed on kilometre-scales.

## 5. Conclusions

The E–W-trending CaSSS (and associated CzSSS) form a sub-vertical, anastomosing array of sigmoidal, mainly brittle fault zones that cut the Amazon Craton in Brazil. They formed in the Late Archaean by reactivation of pre-existing ductile basement fabrics. An early, postulated phase of dextral movements downfaulted low grade to unmetamorphosed cover sequence rocks into dilational jogs, bends and offsets along the CaSSS. These dilation zones were then deformed and partially inverted during a regional episode of sinistral transpression, especially along the CFZ.

The unmetamorphosed sandstone-dominated sequences of the Águas Claras formation are the youngest rocks affected by sinistral transpressional deformation. They display structural features consistent with tectonic deformation prior to complete lithification and thereby constrain the age of sinistral movements to ca. 2.6 Ga.

In the Águas Claras River valley area, the main zone of deformation is focused into a ca. 800-m-wide zone of high strain adjacent to the main trace of the CFZ. A complex zone of disharmonic, curvilinear folds is closely associated with linked sets of steeply dipping sinistral faults and moderately- to shallowly dipping, top-to-the-SW thrusts. Collectively, these folds and faults are interpreted to potentially represent an asymmetric flower structure.

Small-scale kinematic partitioning of the strike-slip and contractional components of the transpressional strain has occurred in the folded and faulted zone along the CFZ. This can, in part, be linked to the progressive rotation of bedding in monoclinal fold limbs into steeply dipping orientations that are then favourable for the development of sub-vertical strike-slip faults. Complex curvilinear folds do not form favourable sites for the localisation of faulting. They are thought to form due to either 3-D oblique relationships between rotated bedding and the principal axes of finite strain, or due to localised superimposed folding events during temporal partitioning of transpressional strain.

Many of these features bear comparison with structures found in the vicinity of upper crustal transpression zones in more modern settings, notably the San Andreas fault zone (e.g. Wilcox et al., 1973; Sylvester and Smith, 1976). This suggests that the architecture and underlying dynamic controls of structural development in upper crustal, obliquely convergent zones have been similar for at least the last 2.6 Ga.

## Acknowledgements

RVLP acknowledges CAPES (Federal Agency for

Postgraduate Education, Brazil) for funding of his PhD and both authors thank CVRD (Companhia Vale do Rio Doce) and the Centro de Geociências, Universidade Federal do Pará for their financial and logistical support. J. Hippertt, D. Cunningham and J. Evans are thanked for their thorough, helpful and constructive reviews.

## References

Alsop, G.I., Holdsworth, R.E., 1999. Vergence and facing patterns in large-scale sheath folds. Journal of Structural Geology 21, 1335–1349.

Araújo, O.J.B. de, Maia, R.G.N., 1991. Projeto especial mapas de recursos minerais, de solos e de vegetação para a área do Programa Grande Carajás; Subprojeto Recursos Minerais; Folha SB.22-Z-A Serra dos Carajás-Estado do Pará. DNPM/CPRM, Brasilia, 136 pp.

Carreras, J., Estrada, A., White, S.H., 1977. The effect of folding on the *c*-axis fabrics of a quartz mylonite. Tectonophysics 39, 3–24.

Costa, J.B.S., Pinheiro, R.V.L., Jorge João, X. da S., Araújo, O.J.B. de, 1991. Esboço estrutural do Proterozóico Médio da Amazônia Oriental. Boletim do Museu Paraense Emílio Goeldi. Série Ciências da Terra 3, 9–24.

Costa, J.B.S., Pinheiro, R.V.L., Bemerguy, R.L., Borgues, M.da S., Costa, A.R., Travassos, W., Mioto, J.A., Igreja, H.L.S. da, 1993. Aspectos fundamentais da neotectonica na Amazonia Brasileira. I Simposio Internacional do Quaternario da Amazonia, Resumos e Contribuicoes Cientificas, Manaus, 103-106.

Curtis, M.L., 1999. Structural and kinematic evolution of a Miocene to Recent sinistral restraining bend: the Montejunto massif, Portugal. Journal of Structural Geology 21, 39–54.

Dall'Agnol, R., Bettencourt, J.S., João, X. da S.J., Medeiros, H. de, Costi, H.T., Macambira, M.J.B., 1987. Granitogenesis in northern Brazilian region: a review. Revista Brasileira de Geologia 17 (4), 382–403.

Dewey, J.F., Holdsworth, R.E., Strachan, R.A., 1998. Transpression and transtension zones. In: Holdsworth, R.E., Strachan, R.A., Dewey, J.F. (Eds.), Continental Transpressional and Transtensional Tectonics, Special Publication of the Geological Society of London, 135, pp. 1–14.

Dias, G.S., Macambira, M.J.B., Dall'Agnol, R., Soares, A.D.V., Barros, C.E. de, 1996. Datação de zircões de sill de metagabro: comprovação da idade arqueana da Formação Águas Claras, Carajás-Pará. V Simpósio de Geologia da Amazônia, SBG-NO, Boletim de Resumos Expadidos, Belém, 376-379.

DOCEGEO, 1988. Revisão litoestratigráfica da Província Mineral de Carajás. Anais XXXV Congresso Brasileiro de Geologia, anexo, Belém, 10-54.

Dooley, T.P., McClay, K.R., 1996. Strike-slip deformation in the Confidence Hills, southern Death Valley fault zone, eastern California. Journal of the Geological Society of London 153, 375–387.

Elliott, C.G., Williams, P.F., 1988. Sediment slump structures: a review of diagnostic criteria and application to an example from Newfoundland. Journal of Structural Geology 10, 171–182.

Flinn, D., 1962. On folding during three-dimensional progressive deformation. Journal of the Geological Society 118, 385–433.

Harding, T.P., 1974. Petroleum traps associated with wrench faults. American Association of Petroleum Geologists Bulletin 58, 1290–1304.

Hobbs, B.E., Means, W.D., Williams, P.F., 1976. An Outline of Structural Geology. John Wiley and Sons, New York.

Holdsworth, R.E., Butler, C.A., Roberts, A.M., 1997. The recognition of reactivation during continental deformation. Journal of the Geological Society of London 154, 73–78.

Laney, S.E., Gates, A.E., 1996. Three-dimensional shuffling of horses in a strike-slip duplex: an example from the Lambertville sill, New Jersey. Tectonophysics 258, 53–70.

Le Pichon, X., Haynes, D.E., 1971. Marginal offsets, fracture zones and the early opening of the South Atlantic. Journal of Geophysical Research 76, 6283–6293.

Machado, N., Lindenmayer, D., Lindenmayer, Z., 1988. Geocronologia U–Pb da Província Metalogenética de Carajós, Pará: resultados preliminares. Anais VII Congresso Latino Americano de Geologia, Belém 1, 339–347.

Machado, W., Lindenmayer, Z., Krogh, T.E., Lindenmayer, D., 1991. U–Pb geochronology of Archean magmatism and basement reactivation in the Carajás area, Amazon shield, Brazil. Precambrian Research 49, 329–354.

Maltman, A.J., 1984. On the term 'soft-sediment deformation'. Journal of Structural Geology 6, 589–592.

Maltman, A.J., 1994. Deformation structures preserved in rocks. In: Maltman, A.J. (Ed.), The Geological Deformation of Sediments. Chapman and Hall, London, pp. 261–307.

Nogueira, A.C.R., 1995. Análise faciológica e aspectos estruturais da Formação Águas Claras, Região Central da Serra dos Carajás-Pará. Unpublished MSc. dissertation, Universidade Federal do Pará, Curso de Pós-Graduação em Geociências, Belém, 167 pp.

Nogueira, A.C.R., Truckenbrodt, W., Pinheiro, R.V.L., 1995. Formação Águas Claras, Pré-Cambriano da Serra dos Carajás. Redescrição e redefinição. Boletim do Museu Paraense Emílio Goeldi. Série Ciências da Terra 7, 177–197.

O'Driscoll, E.S.T., 1986. Observations of the lineament–ore relation. Philosophical Transactions of the Royal Society of London A317, 195–218.

Pinheiro, R.V.L., 1997. Reactivation history of the Carajás and Cinzento Strike Slip Systems, Amazon, Brazil. Unpublished PhD Thesis, Durham, UK, 408 pp.

Pinheiro, R.V.L., Holdsworth, R.E., 1996. Significado tectônico da clivagem transversa (transecting cleavage) em dobras na mina de Serra Pelada, Pará. Boletim do Museu Paraense Emílio Goeldi. Série Ciências da Terra 7, 259–278.

Pinheiro, R.V.L., Holdsworth, R.E., 1997a. Reactivation of Archaean strike-slip fault systems, Amazon region, Brazil. Journal of the Geological Society of London 154, 99–103.

Pinheiro, R.V.L., Holdsworth, R.E., 1997b. The structure of the Carajas N-4 Ironstone deposit and associated rocks: relationship to Archaean strike-slip tectonics and basement reactivation in the Amazon region, Brazil. Journal of South American Earth Sciences 10, 305–319.

Ramsay, J.G., 1967. Folding and Fracturing of Rocks. McGraw-Hill, New York.

Rios, F.J., 1991. O Granito Central da Serra dos Carajás: fácies petrográficas e alteração hidrotermal do setor norte. Unpublished MSc. dissertation, Universidade Federal do Pará, Curso de Pós-Graduação em Geociências, Belém, 152 pp.

Sanderson, D.J., Marchini, W.R.D., 1984. Transpression. Journal of Structural Geology 6, 449–458.

Siqueira, J.B., 1990. Organização lito-estrutural do duplex Salobo–Mirim, Serra dos Carajás. MSc. Dissertation, Universidade Federal do Pará, Curso de Pós-Graduação em Geociências, Belém, Brazil, 125 pp.

Silva, G.G., Lima, M.J.C., Andrade, A.R.F., Issler, R.S., Guimarães, G., 1974. Geologia das folhas SB-22 Araguaia e parte SC-22 Tocantins, Projeto RADAMBRASIL, geologia, geomorfologia, solos e uso potencial da terra, Levantamento de Recursos Naturais (4), Rio de Janeiro, 143 pp.

Stearns, D.W., 1978. Faulting and forced folding in the Rocky Mountains foreland. Memoir of the Geological Society of America 151, 1–37.

Sutton, J., Watson, J.V., 1986. Architecture of the continental lithosphere. Philosophical Transactions of the Royal Society of London A317, 5–12.

Sylvester, A.G., Smith, R.R., 1976. Tectonic transpression and basement controlled deformation in San Andreas Fault Zone, Salton Trough, California. American Association of Petroleum Geologists Bulletin 30, 2981–3102.

Treagus, J.E., Treagus, S.H., 1981. Folds and the strain ellipsoid: a general model. Journal of Structural Geology 3, 1–17.

White, S.H., Bretan, P.G., Rutter, E.H., 1986. Fault-zone reactivation: kinematics and mechanisms. Philosophical Transactions of the Royal Society of London A317, 81–97.

Wilcox, R.E., Harding, T.P., Seeley, D.R., 1973. Basic wrench tectonics. American Association of Petroleum Geologists Bulletin 57, 74–96.

Wirth, K.R., 1986. The geology and geochemistry of the Grão Pará Group, Serra dos Carajás, Pará, Brazil. Unpublished MSc. dissertation, Cornell, Ithaca, New York, 284 pp.

Wirth, K.R., Gibbs, A.K., Olszewski, Jr., 1986. U–Pb ages of zircons from the Grão–Pará Group and Serra dos Carajás Granite, Pará, Brazil. Revista Brasileira de Geociências 16 (2), 195–200.